A study of natural convection above a line fire

By SHAO-LIN LEE

Department of Mechanical Engineering, North Carolina State College

AND H. W. EMMONS

Pierce Hall, Harvard University

(Received 17 April 1961)

The behaviour of a natural convection plume above a line fire is studied both theoretically and experimentally. In the theoretical treatment, a turbulent plume above a steady two-dimensional finite source of heated fluid in a uniform ambient fluid is investigated. By the use of the lateral entrainment assumption, a quadrature solution has been obtained for each of two separate ranges of a source Froude number, $F > 1$ or $F < 1$. In neither of these cases can the finite width line source be accurately represented by an equivalent mathematical line source at a lower level. Only the special case, $F = 1$, can be so represented and its solution is discussed.

In the experimental treatment, hot gases, resulting from the burning of a liquid fuel in a long channel burner, are driven upwards by buoyancy and gradually cooled down by the entrainment of ambient air. The average temperature along lines parallel to the channel burner was measured by a piece of resistance wire. For the case of a non-luminous diffusion flame, the effective radiation loss to the surroundings was assumed to be negligible, and, by a comparison of the energy flux supplied from the fuel and the energy flux contained in the plume, the characteristic turbulence entrainment coefficient is determined. By the alternate use of either an absorbing or a reflecting surface for the table-top surrounding a luminous flame, a measurement was made of the energy radiated from the flame that was intercepted by the fire surroundings and subsequently returned to the buoyancy plume by heating the ingested air. These measurements agree with estimates computed from such data as are available. The experimental results relating to the behaviour of the convection plume agree closely with the theoretical predictions in all cases.

1. Introduction

A line fire exhibits a complex interaction of diverse phenomena. Hot combustion products are driven upwards by natural convection, thus inducting air and fuel for further combustion. Heat is transferred downward by various mechanisms to maintain the combustion temperature in the fresh fuel and air and, if the fuel is liquid, to continue the evaporation process. Simultaneously, interchange of energy between the fire and the various elements of its environment also occur. One of the effects of this phenomenon is the instability of the inflowing air, which results from heat transferred from luminous flames to the surrounding

surface by radiation and thence to the inducted air by conduction and convection as noted by Emmons (1959).

No attempt is made to solve the flame-fuel evaporation problem, but rather attention is given only to the natural convection above the flames. Only the turbulent flow régime is considered. Experimentally, measurements are made above the level of the flames while theoretically the whole fire process is replaced by a horizontal source of heat, momentum and energy, infinitely long and of finite width. In the theory presented these may be varied independently. Since the experiments were conducted in the laboratory, the plumes were only a few metres high and atmospheric variations were negligible. The present work, therefore, extends previous work by the inclusion of arbitrary fire width, and arbitrary momentum and energy sources, rather than the line fire only.

2. Theoretical investigation

It is assumed that turbulent flow is fully developed and thus, as a consequence, molecular transfer mechanisms are negligible relative to the turbulent transfer. It is also assumed that local density variations are everywhere small compared to some reference density in the field. Although natural convection of this nature is produced by a source of heat, it is the buoyancy rather than the thermal properties of the flow which is fundamental to the phenomenon. Therefore, although the buoyant force due to density difference is sufficiently great to produce vertical acceleration, the corresponding variation in the mass density of the fluid undergoing acceleration is sufficiently small, in comparison with the density itself, to be neglected in the continuity and energy equations and the inertia term of the momentum equation.

In addition, we make the 'boundary-layer' assumption that transverse accelerations are small in comparison with those in the vertical direction, and that turbulent mixing in the vertical direction is small in comparison with that in the horizontal direction. A consequence of this is that the pressure has essentially no horizontal variation.

Let the origin O represent the location of the centre of a two-dimensional finite source of width b_0 (accurately defined by equation (8) applied at $x = 0$). The local mean component of velocity in the vertical direction x is denoted by u, and that in the y-direction (in the horizontal plane, normal to the fire) is denoted by v.

Under the foregoing assumptions the fundamental equations of motion reduce to the equation of continuity

$$\frac{\partial u}{\partial x}+\frac{\partial v}{\partial y}=0, \tag{1}$$

the simplified equation of conservation of vertical momentum

$$u\frac{\partial u}{\partial x}+v\frac{\partial u}{\partial y}=\frac{\Delta\gamma}{\rho_1}+\frac{1}{\rho_1}\frac{\partial \tau}{\partial y}, \tag{2}$$

and the simplified equation of conservation of energy

$$u\frac{\partial(\Delta T)}{\partial x}+v\frac{\partial(\Delta T)}{\partial y}=\frac{1}{\rho_1 C_p}\frac{\partial w}{\partial y}. \tag{3}$$

Here ρ_1 is the mass density of undisturbed ambient fluid, and

$$\Delta\gamma = g\Delta\rho = g(\rho_1 - \rho)$$

is the local buoyancy, where ρ is the local mass density, γ the local weight density, and g the gravitational acceleration. Also, $\tau = -\rho_1\overline{u_f v_f}$ is the Reynolds stress, u_f, v_f being fluctuating velocities in the x- and y-directions respectively; $\Delta T = T - T_1$, where T is the local time-mean temperature, and T_1 the temperature of undisturbed ambient fluid. Lastly, C_p is the specific heat at constant pressure, and $w = -\rho_1 C_p \overline{v_f \Delta T_f}$ is the eddy heat transfer, where ΔT_f is the fluctuating temperature difference.

Since $v = 0$ at $y = 0$ by symmetry, integration of equation (1) with respect to y gives

$$\frac{d}{dx}\int_0^\infty u\,dy + v(x,\infty) = 0. \tag{4}$$

This equation states that the increase of ascending mass in a heated plume is due to the lateral entrainment of the ambient fluid.

Since no work is applied at either $y = 0$ or $y = \infty$ and the flow is symmetrical with respect to $y = 0$, therefore $\tau = 0$ at both $y = 0$ and $y = \infty$. Integration of equation (2) with respect to y by parts, with use of equation (1), gives

$$\frac{d}{dx}\int_0^\infty u^2 dy = \int_0^\infty \frac{\Delta\gamma}{\rho_1} dy. \tag{5}$$

This equation states that the increase of vertical momentum of ascending mass of heated fluid is due to the buoyancy effect caused by the density difference.

Since no heat is added at either $y = 0$ or $y = \infty$ and the flow is symmetrical with respect to $y = 0$, therefore $w = 0$ at both $y = 0$ and $y = \infty$. By the assumption that the ambient fluid is undisturbed, $\Delta T = 0$ at $y = \infty$. Integration of equation (3) with respect to y, using equation (1) and the assumption of small density variation, gives

$$\frac{d}{dx}\int_0^\infty u\Delta\gamma\,dy = 0. \tag{6}$$

This equation states that the buoyancy flux of an ascending mass of heated fluid is conserved.

When a stream of fluid is in contact with another stream, the eddies which cause transfer of matter between them are characterized by velocities proportional to the relative velocity of the two streams. This can be seen from dimensional considerations, since if the mutual entrainment is turbulent the only quantity determining the motion is the relative velocity of the two streams. This was also shown by the experiment of Kuethe (1935) on the mixing at the edge of a jet. The rate at which the bounding edge of a heated plume expands and absorbs the surrounding fluid into the plume may similarly be assumed proportional to the velocity at that level. As first suggested by Taylor (1945) and later adopted by Morton, Taylor & Turner (1956) and Morton (1959), the rate at which fluid is entrained into the heated plume is taken as proportional to the vertical velocity on the axis of the plume, thus

$$v(x,\infty) = \alpha u(x,0), \tag{7}$$

where α is the entrainment constant.

Rouse, Yih & Humphreys (1952) have obtained velocity and temperature measurements of heated plumes above a line of small gas flames designed to simulate a line heat source. Their results show the Gaussian profiles

$$\exp(-32y^2/x^2) \quad \text{and} \quad \exp(-41y^2/x^2)$$

for the velocity and temperature measurements, respectively. Since the entrainment constant α is by definition associated with the velocity profile rather than the temperature profile, it will be appropriate to seek a similarity solution for which α measures the rate of flow into a heated plume, with velocity profile characterized by a horizontal length-scale b, and with an associated buoyancy profile of the same shape but with a length-scale λb. α and λ are assumed to be universal constants.

Consider a two-dimensional heated plume generated from a finite source in an incompressible environment. The plume will be assumed to have Gaussian profiles of time-mean vertical velocity and time-mean buoyancy: thus

$$u(x,y) = u(x)\exp(-y^2/b^2), \tag{8}$$

where $u(x) = u(x,0)$ is the time-mean vertical velocity on the axis of symmetry of the plume, and

$$\Delta\gamma(x,y) = \Delta\gamma(x)\exp(-y^2/\lambda^2 b^2), \tag{9}$$

where $\Delta\gamma(x) = \Delta\gamma(x,0)$ is the time-mean buoyancy on the plume axis. The finite source will be characterized by $b(0) = b_0$, $u(0) = u_0$ and $\Delta\gamma(0) = \Delta\gamma_0$. Substituting equations (8) and (9) into equations (4), (5) and (6), we have the equations of continuity, conservation of vertical momentum and conservation of energy

$$\frac{d}{dx}[ub] = \frac{2}{\pi^{\frac{1}{2}}}\alpha u, \tag{10}$$

$$\frac{d}{dx}[u^2 b] = 2^{\frac{1}{2}}\lambda g b\frac{\Delta\gamma}{\gamma_1}, \tag{11}$$

$$\frac{d}{dx}[ub\Delta\gamma] = 0, \tag{12}$$

subject to the boundary conditions

$$b = b_0, \quad u = u_0, \quad \Delta\gamma = \Delta\gamma_0 \quad \text{at} \quad x = 0. \tag{13}$$

With the following transformations designed to remove all unnecessary coefficients,

$$\left.\begin{aligned} x' &= (2/\pi^{\frac{1}{2}})\alpha x/b_0, \\ b' &= b/b_0, \\ p' &= (\Delta\gamma/\gamma_1)/(\Delta\gamma_0/\gamma_1), \\ u' &= \left(\frac{2^{\frac{1}{2}}}{\pi^{\frac{1}{2}}}\frac{1}{g}\frac{\alpha}{\lambda}\frac{1}{b_0}\frac{\gamma_1}{\Delta\gamma_0}\right)^{\frac{1}{2}} u, \end{aligned}\right\} \tag{14}$$

we have, from equations (10) to (13), the equations

$$\frac{d}{dx'}[u'b'] = u', \tag{15}$$

$$\frac{d}{dx'}[u'^2 b'] = b'p', \tag{16}$$

$$\frac{d}{dx'}[u'b'p'] = 0, \tag{17}$$

subject to the boundary conditions

$$b' = 1, \quad u' = F, \quad p' = 1 \quad \text{at} \quad x' = 0, \tag{18}$$

where

$$F = \left(\frac{2}{\pi}\right)^{\frac{1}{4}} \left(\frac{1}{g}\frac{\alpha}{\lambda}\frac{1}{b_0}\frac{\gamma_1}{\Delta\gamma_0}\right)^{\frac{1}{2}} u_0.$$

We note that this group can be written

$$F = \left(\frac{2}{\pi}\right)^{\frac{1}{4}} \left(\frac{\alpha}{\lambda}\frac{\gamma_1}{\Delta\gamma_0}\right)^{\frac{1}{2}} \frac{u_0}{(gb_0)^{\frac{1}{2}}},$$

a source Froude number of the usual form $u_0/(gb_0)^{\frac{1}{2}}$ modified by factors $(2/\pi)^{\frac{1}{4}}$ to account for the Gaussian distribution, $(\alpha/\lambda)^{\frac{1}{2}}$ to account for the difference between velocity and buoyancy profiles, and $(\Delta\gamma_0/\gamma_1)^{\frac{1}{2}}$ to account for the actual effective density difference. This Froude number plays an essential role in what follows. Equation (17) can be immediately integrated to give

$$u'b'p' = F, \tag{19}$$

by the use of which equation (16) becomes

$$\frac{d}{dx}[u'^2b'] = \frac{F}{u'}. \tag{20}$$

To solve equations (15) and (20) introduce the 'mass flux' and 'momentum flux' as two new variables

$$N = u'b', \quad M = u'^2b'. \tag{21}$$

Thus we get

$$\frac{dN}{dx'} = \frac{M}{N}, \tag{22}$$

$$\frac{dM}{dx'} = \frac{FN}{M}, \tag{23}$$

subject to the boundary conditions

$$N = F, \quad M = F^2 \quad \text{at} \quad x' = 0. \tag{24}$$

By eliminating x' and integrating, we find that

$$FN^3 = M^3 + c, \tag{25}$$

where $c = F^4(1 - F^2)$. We note that both mass and momentum flux are positive and by equations (22) and (23) increase with increasing x', although c may be zero or have either sign.

The position in the plume is now found by integrating equation (22), i.e.

$$x' = \int_F^N \frac{N\,dN}{M} = \int_F^N \frac{N\,dN}{(FN^3 - c)^{\frac{1}{3}}}. \tag{26}$$

It is convenient to consider separately three cases, $c < 0$, $c = 0$, $c > 0$, and arrange the integral for graphical or numerical evaluation. The three ranges correspond to $F < 1$, $F = 1$, and $F > 1$, respectively.

Case I. $F = 1$, the line source

For $F = 1$, $c = 0$, equations (25) and (26) give

$$N = M \tag{27}$$

and

$$x' = N - I, \tag{28}$$

which together with equations (19) and (21) give

$$u' = 1, \quad b' = x' + 1, \quad p' = \frac{1}{x'+1}. \tag{29}$$

These equations are plotted in figure 1.

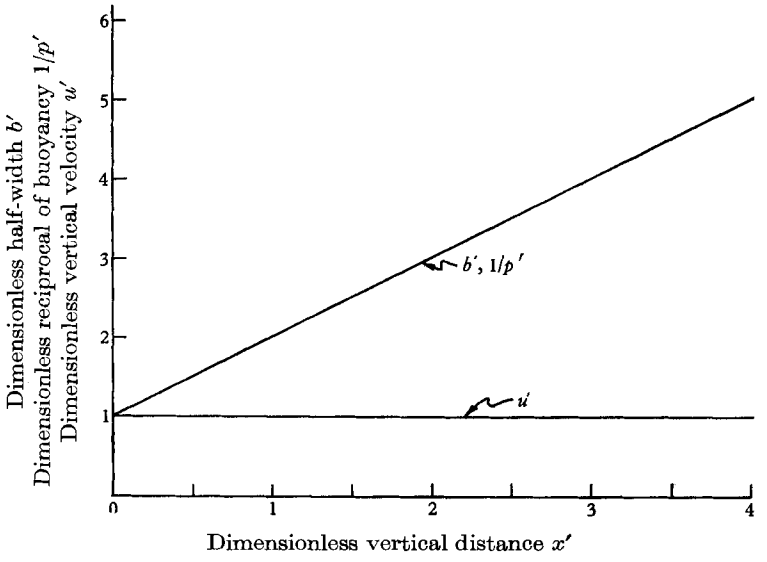

FIGURE 1. Graphical representation of the theoretical solution for a plume issuing from a neutral source, $F = 1$.

If we introduce the conserved buoyancy flux across any horizontal cross-section

$$Q = \int_{-\infty}^{\infty} gu(x,y)\frac{\Delta\gamma(x,y)}{\gamma_1}dy = \pi^{\frac{1}{2}}\frac{\lambda g}{(1+\lambda^2)^{\frac{1}{2}}}F\frac{b_0\Delta\gamma_0}{\gamma_1}, \tag{30}$$

we have, from equation (29), the familiar forms

$$\left.\begin{aligned} u &= \{\tfrac{1}{2}(1+\lambda^2)\}^{1/\gamma}\alpha^{-\frac{1}{3}}Q^{\frac{1}{3}}, \\ b &= 2\pi^{-\frac{1}{2}}\alpha x + b_0, \\ \frac{\gamma_1}{\Delta\gamma} &= \frac{(2)^{\frac{5}{6}}g\lambda\alpha^{\frac{2}{3}}}{(1+\lambda^2)^{\frac{1}{3}}Q^{\frac{2}{3}}}\left(x + \frac{\pi^{\frac{1}{2}}}{2\alpha}b_0\right). \end{aligned}\right\} \tag{31}$$

If some arbitrary point in the plume were regarded as the source at which the convection started, we would compute a source Froude number of $F = 1$ independent of location. Thus, the above solution describes the convection above a line source $b_0 = 0$ in which case the velocity $u = \text{const.}$, the plume 'width' b is proportional to x, while the buoyancy $\Delta\gamma/\gamma_1$ is inversely proportional to x.

Furthermore, for a finite width line source, the whole convection column can be regarded as arising from a line source situated a distance $x_0 = \pi^{\frac{1}{2}} b_0/2\alpha$ below the real source. We note that the equivalent line source has a finite buoyancy flux if $b_0 \Delta\gamma_0$ is constant; i.e. if the density difference becomes infinitely great as the source width goes to zero.

Case II. Plume issuing from a restrained source ($F < 1$)

The integral of equation (26) is expressible as an incomplete beta function. However, direct numerical integration is more convenient. For this purpose the parameters are removed by setting

$$N = \beta\nu, \tag{32}$$

with

$$\beta = \left(\frac{C}{F}\right)^{\frac{1}{3}} = F(1-F^2)^{\frac{1}{3}}.$$

There results

$$x' = \{F^2(1-F^2)\}^{\frac{1}{3}} \int_{\nu_0}^{\nu} \frac{\nu d\nu}{(\nu^3-1)^{\frac{1}{3}}}, \tag{33}$$

where

$$\left.\begin{aligned} \nu &= (1-F^2)^{-\frac{1}{3}} \frac{N}{F}, \\ \nu_0 &= (1-F^2)^{-\frac{1}{3}}. \end{aligned}\right\} \tag{34}$$

These integration limits are both greater than 1, the upper limit being larger than the lower limit. Since for the Froude number limits of this case $F = 0$, $F = 1$, ν has limits of 1 and ∞, we define

$$I_1(\nu) = \int_1^{\nu} \frac{\nu d\nu}{(\nu^3-1)^{\frac{1}{3}}}, \tag{35}$$

and the height scale in the convection plume is given by

$$x' = \{F^2(1-F^2)\}^{\frac{1}{3}} \{I_1(\nu) - I_1(\nu_0)\}. \tag{36}$$

Thus the actual plume may be regarded as a section of the plume arising from a virtual source at a distance $\{F^2(1-F^2)\}^{\frac{1}{3}} I_1(\nu_0)$ below the real source. The strength of the real source is specified by its 'mass flux' $N_0 = F$, while the 'mass flux' increases along the plume as $N = F(1-F^2)^{\frac{1}{3}}\nu$ increases.

From equations (19), (21), (25) and (32), the physically interesting quantities are given as follows:

$$\left.\begin{aligned} &\text{plume half-width} && b' = \{F^2(1-F^2)\}^{\frac{1}{3}} \frac{\nu^2}{(\nu^3-1)^{\frac{1}{3}}}, \\ &\text{velocity} && u' = F^{\frac{1}{3}} \frac{(\nu^3-1)^{\frac{1}{3}}}{\nu}, \\ &\text{buoyancy} && p' = \frac{1}{(1-F^2)^{\frac{1}{3}}\nu}. \end{aligned}\right\} \tag{37}$$

The integral $I_1(\nu)$ was evaluated graphically and the physical plume characteristics are plotted in figure 2. The real plume may be visualized from this figure

by imagining the actual source located at a distance to the right of the origin given by

$$x_0'' = \frac{x_0'}{\{F^2(1-F^2)\}^{\frac{1}{3}}} = I_1\{(1-F^2)^{-\frac{1}{3}}\}, \tag{38}$$

while other higher plume points appear to the right of the actual source. The plume shape is particularly interesting. For a real source with $F < 2^{-\frac{1}{2}}$ the plume width first decreases and then increases again. Furthermore, any plume at great height behaves as though it arose from a line source located at a distance (in the scale of equation (37)) of 0·7 below the virtual origin.

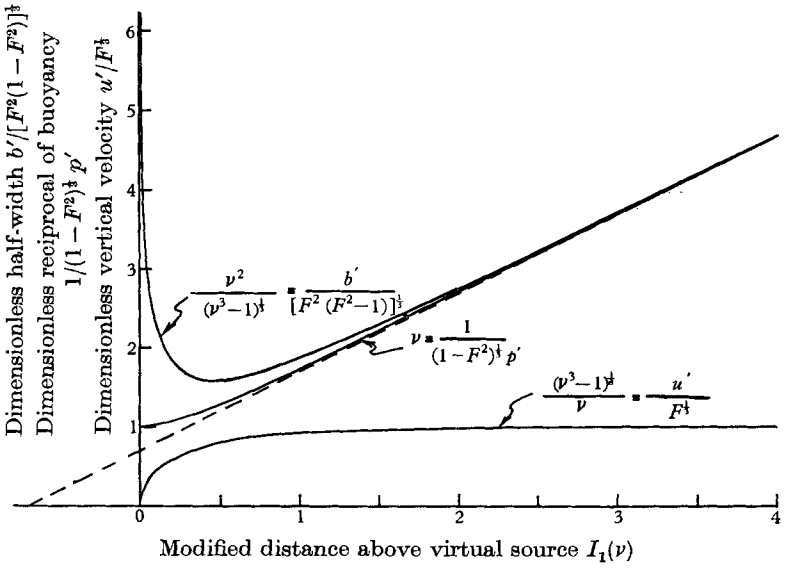

FIGURE 2. Graphical representation of the theoretical solution for a plume issuing from a restrained source (see equation (33)), $F < 1$.

Case III. Plume issuing from an impelled source ($F > 1$)

We again remove the parameters from the integral of equation (26) by setting

$$N = \beta\nu, \tag{39}$$

where now $\beta = F(F^2-1)^{\frac{1}{3}}$.

The resulting integral for graphical evaluation is

$$x' = \{F^2(F^2-1)\}^{\frac{1}{3}} \int_{\nu_0}^{\nu} \frac{\nu d\nu}{(\nu^3+1)^{\frac{1}{3}}}, \tag{40}$$

with

$$\left.\begin{aligned} \nu &= (F^2-1)^{-\frac{1}{3}}\frac{N}{F}, \\ \nu_0 &= (F^2-1)^{-\frac{1}{3}}, \end{aligned}\right\} \tag{41}$$

where $0 < \nu_0 < \nu < \infty$.

For this case we use zero as the lower limit and define

$$I_2(\nu) = \int_0^{\nu} \frac{\nu d\nu}{(\nu^3+1)^{\frac{1}{3}}}, \tag{42}$$

from which the position in the plume is computed as

$$x' = \{F^2(F^2-1)\}^{\frac{1}{3}}\{I_2(\nu)-I_2(\nu_0)\}. \tag{43}$$

By equations (19), (21), (25) and (39), the physically interesting quantities are obtained:

$$\left.\begin{aligned} &\text{plume half-width} && b' = \{F^2(F^2-1)\}^{\frac{1}{3}}\frac{\nu^2}{(\nu^3+1)^{\frac{1}{3}}},\\ &\text{velocity} && u' = F^{\frac{1}{3}}\frac{(\nu^3+1)^{\frac{1}{3}}}{\nu},\\ &\text{buoyancy} && p' = \frac{1}{(F^2-1)^{\frac{1}{3}}\nu}. \end{aligned}\right\} \tag{44}$$

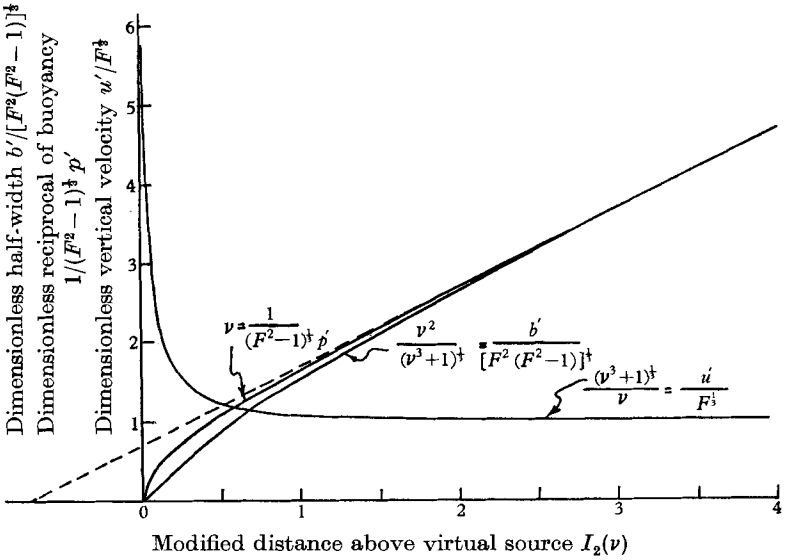

FIGURE 3. Graphical representation of the theoretical solution for a plume issuing from an impelled source (see equation (43)), $F > 1$.

Curves of these plume properties are given in figure 3. Again the origin of the distance scale may be regarded as a virtual source with the real source located at a distance

$$x_0'' = \frac{x_0'}{\{F^2(F^2-1)\}^{\frac{1}{3}}} = I_2\{(F^2-1)^{\frac{1}{3}}\}, \tag{45}$$

and the real plume given by the curves from the real source to infinity. The plume grows in size rapidly at first and then more and more slowly. In this case too, the plume at great heights becomes like the plume from a line source located at a distance of 0·7 below the *virtual* source.

We note that both cases II and III approach the case of $F = 1$ as height increases. $F = 1$ corresponds to a balance between inducted mass increase and buoyancy which just maintains the vertical velocity constant. If the plume velocity is relatively too small, i.e. $F < 1$, the plume grows slowly or even contracts to raise the local Froude number. If, on the other hand, the plume velocity is too high, as in a heated jet, i.e. $F > 1$, the plume grows more rapidly, decreasing the velocity.

3. Experimental investigation

The channel burner, 0·564 in. wide, 0·282 in. deep and 78 in. long, is cooled on the sides by a water-jacket, which controls the fuel consumption rate, and is connected by inlets underneath to a metered steady fuel supply system. On either side of the channel burner there is an 18 in. wide asbestos side plate set flush with the sides of the channel burner to prevent any entrainment of air from below. Against each end of the channel burner stands a vertical asbestos end plate to prevent the entrainment from the ends. A view of the apparatus is shown as figure 4 (plate 1). Except for cases with very low fuel consumption rates, the flame from the channel burner fluctuates both with time and location along the length of the channel burner. The average temperature at different heights was measured with a 40 in. piece of pure nickel resistance wire 0·002 in. in diameter suspended parallel to the channel burner. Two fuels were chosen, acetone and methyl alcohol, because they differ considerably from one another in radiation from the flames. Two different kinds of surface were chosen for the side plates, aluminium foil surface and bare asbestos surface, because they react very differently to radiation.

(*A*) *Analyses of asymptotic behaviour of plumes*

For either methyl alcohol or acetone, Gaussian profiles of the natural convection plume are found to prevail at all measurable heights and the corresponding values of the characteristic buoyancy half-width are thus computed. For each plume the values of the slopes $d(\gamma_1/\Delta\gamma)/dx$ and $d(\lambda b)/dx$ were obtained graphically from the measured centre-line buoyancy and Gaussian width respectively and are found to approach their respective asymptotic values.

These asymptotic values are given in a convenient form by equation (31)

$$\left.\begin{aligned}\left[\frac{d(\gamma_1/\Delta\gamma)}{dx}\right]_{\lim} &= \frac{(2)^{\frac{5}{3}}g\lambda\alpha^{\frac{2}{3}}}{(1+\lambda^2)^{\frac{1}{3}}Q^{\frac{2}{3}}},\\ \left[\frac{d(\lambda b)}{dx}\right]_{\lim} &= 2\pi^{-\frac{1}{2}}\alpha\lambda.\end{aligned}\right\} \tag{46}$$

The energy flux Q in this equation could be computed from the rate of fuel use and the fuel properties if it were not for radiation losses. If radiation is negligible, the energy flux from the fuel $\bar{Q}$ is

$$\bar{Q} = \frac{qg(H-\delta h)}{C_p\rho_1 T_1}, \tag{47}$$

where q represents the mass consumption rate of fuel per unit length of burner, H the heat of combustion per unit mass of fuel, and δh the heat removed by the cooling water per unit mass of fuel burned.

(*a*) *Convection plumes above a non-luminous diffusion flame of methyl alcohol*

Since radiation is relatively unimportant in the process of heat transfer from a non-luminous flame, the surface condition of the side plates would be expected to have relatively little effect on the behaviour of the convection plume above

the flame. Experiments with asbestos board side plates and bright aluminium foil side plates gave nearly identical convection plumes with the methyl alcohol flames. Thus the heat released from chemical reaction minus the amount removed by cooling water is carried away by the convection plume and Q equals $\bar{Q}$. Therefore the values of the assumed universal constants α and λ can be computed from equation (46) and the asymptotic data. We find $\alpha = 0{\cdot}16$, $\lambda = 0{\cdot}9$, which check very well with values computed from results of velocity and temperature measurements by Rouse *et al.* (1952) from natural convection plumes above a simulated line buoyancy source. Furthermore, the value of α also checks very well with a value computed from velocity measurements of a turbulent two-dimensional free jet by Reichardt (1942).

(*b*) *Convection plumes above a luminous diffusion flame of acetone*

Since in a luminous flame carbon particles radiate energy to the surroundings, the value of Q in the convection plume is usually smaller than that of $\bar{Q}$. The difference $\bar{Q}-Q$ is the net radiation loss from the flame-plume system to the surroundings. The results of experimental measurements with asbestos and with aluminium side plates are shown in figure 5.

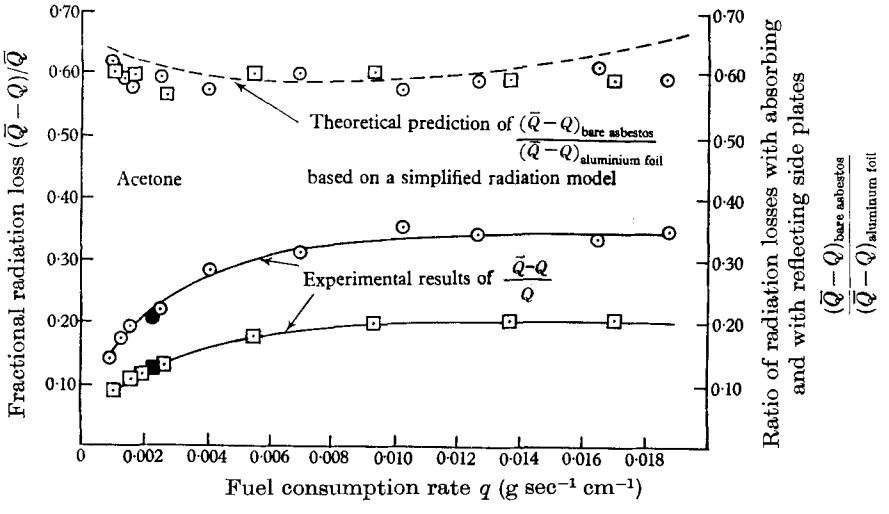

FIGURE 5. Radiation loss computed from measurements of the plume above a luminous diffusion flame of acetone: ⊡, with bare asbestos side plates; ⊙, with aluminium foil-covered side plates (estimates based on average temperature of carbon particles and emissivity measured by Tankin 1960).

It is readily seen that the net loss to the surroundings is lower for the case with bare asbestos side plates, than for those covered with aluminium foil. This can be explained by the difference in the way radiant energy is dealt with by the surface of the side plates in the two cases. The bare asbestos surface has a very high emissivity ($\epsilon = 0{\cdot}96$) and thus absorbs almost all of the radiant energy from the flame intercepted by it. The asbestos surface thus heated will give up heat by conduction to the adjacent air, which is then convected into the flame-plume. On the other hand, the aluminium foil surface has a very low emissivity

($\epsilon = 0{\cdot}087$) and will reflect almost all of the radiant energy from the flame intercepted by it. Thus all radiation from the flame not directly intercepted by the fuel is permanently lost from the convection column.

To estimate the flame radiation loss, use is made of measurements by Tankin (1960) with a bolometer of the average temperature of flame carbon particles, and of the emissivity of a luminous diffusion flame of acetone. A simplified line radiation source was used to estimate the radiation loss of a flame of approximately the same brightness, over the channel burner. The results, shown as solid points in figure 5, are in good agreement with findings of the plume measurements. The ratio of radiation losses with absorbing and with reflecting side plates based on the same simplified radiation model, is also shown in figure 5 as the broken curve which checks quite well with findings of the plume measurements at all values of fuel consumption rate.

(*B*) *Comparison of theoretical and experimental convection plume results*

It is predicted by the theoretical analysis that the behaviour of a plume above a finite source depends on a parameter F which is a function of the source characteristics, b_0, u_0 and $\Delta\gamma_0/\gamma_1$. It is then desirable to determine the values of F by comparing the theoretical predictions with the experimental data.

It is seen from figures 2 and 3 that the solutions for the variation of plume half-width with vertical distance and the location of the actual source above a virtual source, when all dimensionless quantities are converted back to physical quantities, depend only on two of the three independent characteristics of the source, F and b_0. For an origin assumed to be at the mean flame height, experimental data on the plume half-width are plotted against theoretical predictions based on different pairs of trial values of F and b_0. By the principle of least squares, the best-fit values of F and b_0 are determined for each case. The corresponding best-fit value of $\Delta\gamma_0/\gamma_1$ is then determined by comparing the theoretical predictions and experimental data on the variation of buoyancy with vertical distance. The values of F thus found for an origin assumed to be at the mean flame height are listed in table 1.

The plumes from a methyl alcohol flame are seen to lie in the region of $F < 1$, while the plumes from an acetone flame are found to lie in the region of $F < 1$ for low burning rates and $F > 1$ for high burning rates. Very good agreement has been found between theoretical predictions and experimental measurements for all the experiments performed as shown by the sample comparisons made in figures 6 and 7.

(*C*) *Interpretation of experimental results with the introduction of a simplified flame model*

The rigorous analysis of a flame is extremely complicated. However, if the main interest is in the study of the convection plume then the flame itself serves merely as a supplier of heated fluid to the source at the mean flame height for the convection problem. Therefore, if we introduce a simplified flame model with uniform temperature and vertical velocity distributions along a mean flame contour as shown in figure 8, the characteristics of the source can be determined.

Based on such a simplified flame model, the energy flux from the flame is

$$Q = 2g\bar{b}_0 u_0 \frac{\Delta\gamma_0}{\gamma_1}, \tag{48}$$

where $\bar{b}_0$ is the half-channel width of the inside burner. The energy flux contained in the plume, from equation (30), is

$$Q = (\pi)^{\frac{1}{2}} \frac{\lambda g}{(1+\lambda^2)^{\frac{1}{2}}} b_0 u_0 \frac{\Delta\gamma_0}{\gamma_1}. \tag{49}$$

Fuel	Side plates	q (g sec^{-1} cm^{-1})	F
Acetone	Bare asbestos	0·00110	0·79
		0·00163	0·98
		0·00191	1·33
		0·00268	1·83
		0·0055	3·56
		0·0093	5·85
		0·0138	8·67
		0·0170	10·7
Acetone	Aluminium foil	0·00100	0·65
		0·00134	0·85
		0·00157	0·98
		0·00254	1·49
		0·0041	2·14
		0·0070	3·74
		0·0103	5·37
		0·0127	6·75
		0·0165	8·82
		0·0187	10·3
Methyl alcohol	Bare asbestos	0·000716	0·39
		0·000885	0·48
		0·00158	0·85
Methyl alcohol	Aluminium foil	0·0074	0·40
		0·00158	0·85

TABLE 1. Values of Froude number at the effective source obtained from plume measurements.

Comparing equations (48) and (49), we have

$$b_0 = \frac{2}{(\pi)^{\frac{1}{2}}} \frac{(1+\lambda^2)^{\frac{1}{2}}}{\lambda} \bar{b}_0. \tag{50}$$

Eliminating u_0 and b_0 among equations (18), (49) and (50), we then have

$$F = \frac{\alpha^{\frac{1}{2}}}{(2)^{\frac{1}{4}} g^{\frac{3}{2}} (1+\lambda^2)^{\frac{1}{4}}} \frac{1}{\bar{b}_0^{\frac{3}{2}}} \left(\frac{\gamma_1}{\Delta\gamma_0}\right)^{\frac{3}{2}} Q. \tag{51}$$

The values of F of the source computed from equation (51) with such data as available check closely with those determined from plume measurements as shown by the sample comparison in figure 9.

4. Conclusions

(*a*) *Theoretical conclusions*

A quadrature solution for a two-dimensional turbulent natural convection plume above a finite source has been obtained with the assumptions of lateral entrainment and similar Gaussian velocity and temperature profiles. A characteristic parameter F based on the characteristics of the finite source, has been found to describe the behaviour of the plume above that source. Plumes for cases where $F < 1$ and $F > 1$ behave differently but both approach asymptotically the case where $F = 1$. The solution for the case where $F = 1$ is identified as the solution for a plume above a line buoyancy source situated at a lower level.

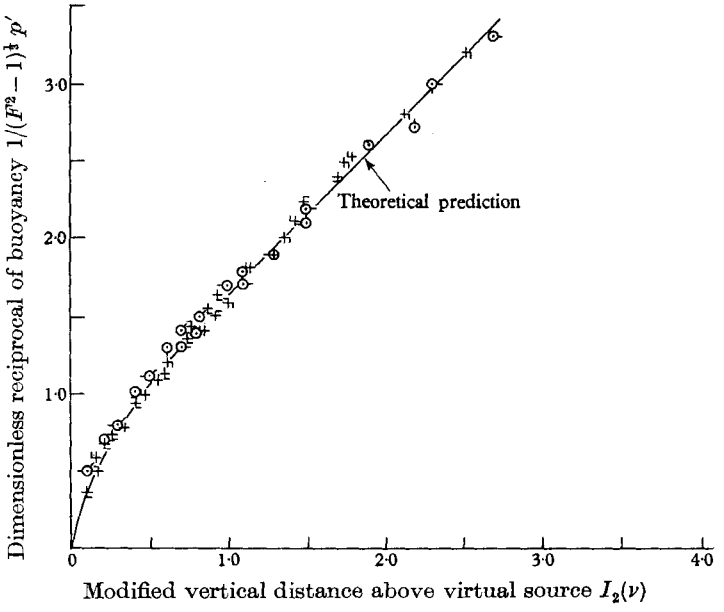

FIGURE 6. Example of comparison between theoretical and experimental results for the buoyancy in the plume above an acetone flame, $F > 1$.

	q (g sec^{-1} cm^{-1})	F		q (g sec^{-1} cm^{-1})	F
Bare asbestos side plates	0·00191	1·33	Side plates covered with aluminium foil	0·00254	1·49
	0·00268	1·83		0·0041	2·14
	0·0055	3·56		0·0070	3·74
	0·0093	5·85		0·0103	5·37
	0·0138	8·67		0·0127	6·75
	0·0170	10·70		0·0165	8·82
				0·0187	10·33

(*b*) *Experimental conclusions*

(i) A Gaussian profile was found to prevail at all measurable heights.

(ii) Values of the entrainment constant α and the auxiliary constant λ obtained from methyl alcohol burnings agree closely with those evaluated from the previously established data.

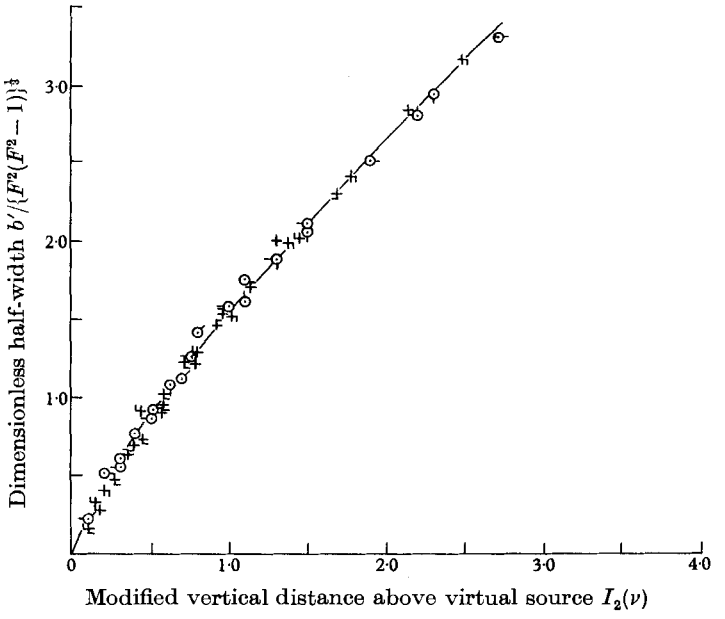

FIGURE 7. Example of comparison between theoretical and experimental results for the half-width of the plume above an acetone flame, $F > 1$. The theoretical curve is drawn in a continuous line.

		q (g sec^{-1} cm^{-1})	F
Bare asbestos side plates	⊙	0·00191	1·33
	⊙	0·00268	1·83
	⊙	0·0055	3·56
	⊙	0·0093	5·85
	⊙	0·0138	8·67
	⊙	0·0170	10·70

		q (g sec^{-1} cm^{-1})	F
Side plates covered with aluminium foil	+	0·00254	1·49
	+	0·0041	2·14
	+	0·0070	3·74
	+	0·0103	5·37
	+	0·0127	6·75
	+	0·0165	8·82
	+	0·0187	10·33

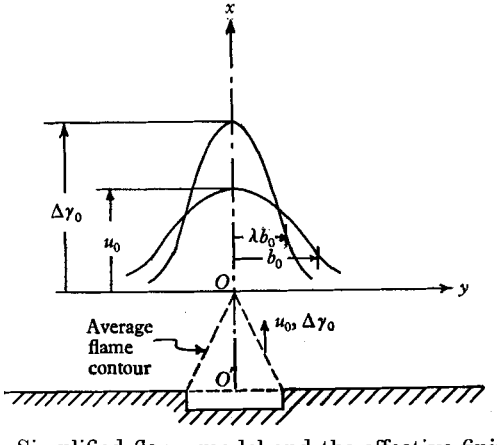

FIGURE 8. Simplified flame model and the effective finite source for the convection plume.

(iii) The radiant heat loss from a luminous flame to its surroundings determined from measurements on convection plumes agrees with estimates computed from such data as are available. The effect the surface condition of the side plates has on the behaviour of the plume from plume measurements checks very well with that from an estimate based on a simplified radiation source.

(iv) Experimental results for the natural convection plumes above a line fire are found in all cases in good agreement with theoretical predictions for the two-dimensional natural convection above a steady finite source of heated fluid. An interpretation is provided by the assumption of an effective source based on a simplified flame model.

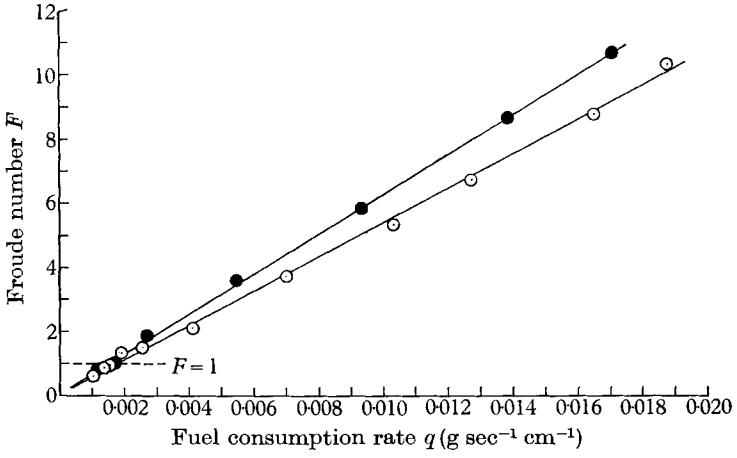

FIGURE 9. Example of comparison between the computed Froude number based on a simplified flame model and the experimentally determined Froude number of an effective source for the convection plume above an acetone flame: ●, with bare asbestos side plates; ⊙, with aluminium foil covered side plates. The two theoretical curves are drawn as continuous lines, the respective curve being the one closest to the experimental results.

REFERENCES

EMMONS, H. W. 1959 *National Fire Research Committee Report.*

KUETHE, A. M. 1935 *Trans. Amer. Soc. Mech. Engrs*, **2**, 87–98.

MORTON, B. R. 1959 *J. Fluid Mech.* **5**, 151–63.

MORTON, B. R., TAYLOR, G. I. & TURNER, J. S. 1956 *Proc. Roy. Soc.* A, **234**, 1–22.

REICHARDT, H. 1942 *VDI-Forschungeheft*, p. 414.

ROUSE, H., YIH, C. S. & HUMPHREYS, H. W. 1952 *Tellus*, **4**, 201–9.

TANKIN, R. S. 1960 Ph.D. Thesis, Harvard University.

TAYLOR, G. I. 1945 U.S. Atomic Energy Commission, MDDC-919, LADC-276.

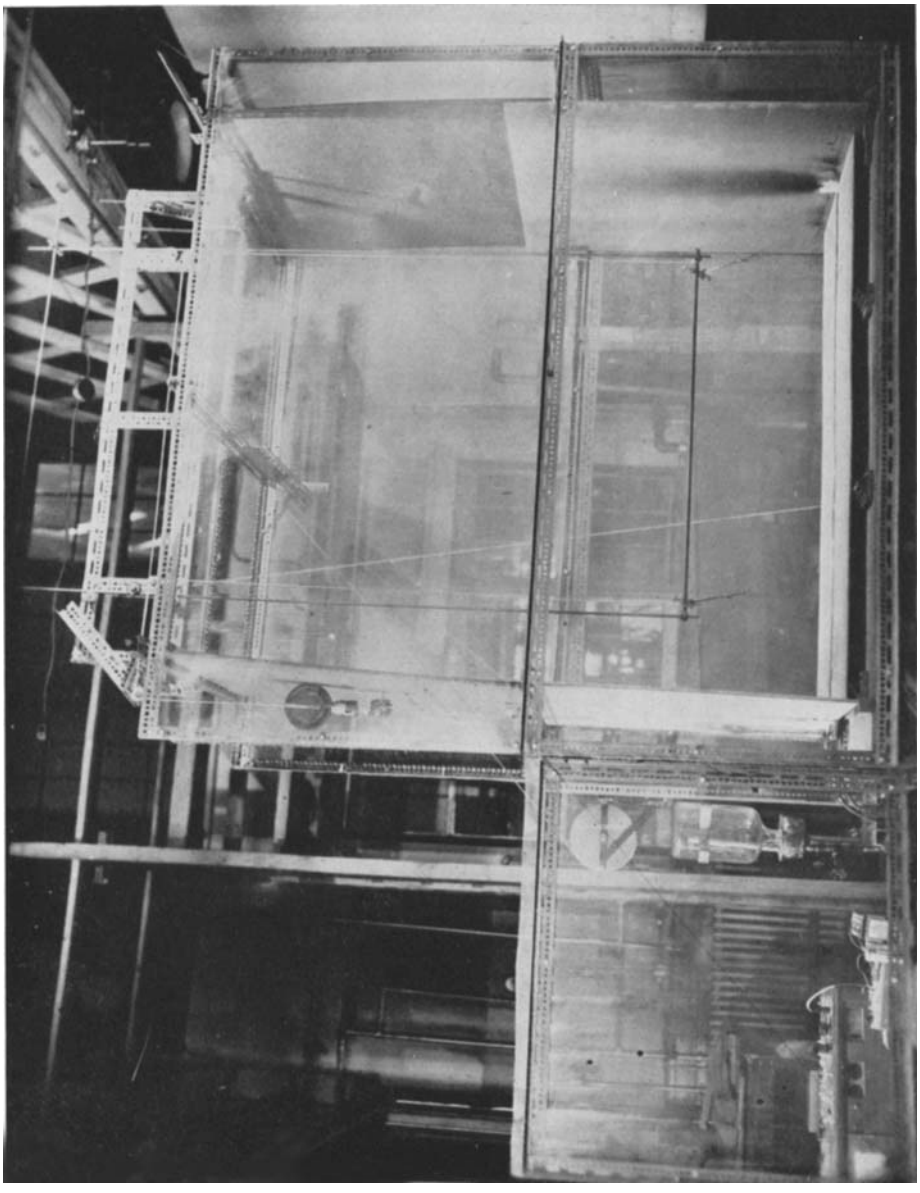

FIGURE 4 (plate 1). Experimental arrangements.